

# Fault Location in Distribution Systems with Distributed Generation

Cansın Y. Evrenosoğlu, Ali Abur

Texas A & M University  
College Station, TX, USA  
abur@ee.tamu.edu

**Abstract** - A travelling wave based fault location technique is presented for radial distribution systems with distributed generation (DG). The proposed technique extracts the fault initiated high frequency components of the voltage signals, which are recorded only at the substation, by using wavelet transformation technique. The simulations show that the technique overcomes the problems encountered in power frequency based fault location techniques and the presence of distributed generation has no significant effect on the scheme. The simulations are carried out by using ATP/EMTP program and the results are processed in MATLAB using Wavelet Toolbox.

**Keywords** - Distributed Generation, Fault Location, Distribution Systems, Protection, Wavelet Transforms, Modal Transformation

## 1 Introduction

RECENT trends in proliferation of distributed generation in distribution systems lead to investigation of protection schemes for such systems. Fault location in distribution systems presents special challenges due to the lack of fault signal recordings at the remote end of the feeders. Typically, fault signals are recorded at the substation and the location of the fault is estimated based on these recordings. Earlier methods rely heavily on power frequency components, which remain sensitive to fault path resistance, line loading and source parameters. Existence of distributed generation causes errors in power frequency based fault location methods which use apparent impedance seen from the substation as a criterion to estimate the distance to the fault point. Such methods also have to deal with the problem of multiple possible locations for a given set of recorded signals. Furthermore, coordination of relays and other protective devices becomes unmanageable by these methods due to infeed currents from distributed generators. Effects of DG on protective device (fuse-fuse, recloser-fuse, relay-relay) coordination are described in [1], [2] and [3].

Traveling wave methods facilitate the estimation of fault location due to the insensitivity of the high frequency components to remote infeed currents from the generator side. Traveling wave based techniques make use of high frequency components of the fault signals and try to capture the arrival times of fault generated transient waves at the line terminals. In [4] a travelling wave based method is proposed for distribution systems with tapped loads. A High Pass Filter (HPF) is used to capture the transients and polarity change is used in order to identify the

faulted region. Another protection scheme for fault detection and location in DG systems is proposed in [5] utilizing wavelet associated Artificial Neural Networks for fault detection and fuzzy cluster analysis for fault location.

In this paper, a travelling wave based fault location method which has been successfully applied to single and double ended fault location problems in transmission systems in [6] and [7], is extended to distribution systems with distributed generation. The paper presents illustrative examples simulated by a transients simulation program for various distribution system configurations. It is shown that faults in distribution systems can be accurately located even when there is generator at the remote ends of the feeder.

## 2 A General Procedure for Fault Location Using Wavelet Transformation

In distribution systems with distributed generation at remote locations, the measurements are only available at the substation. Thus, the fault location procedure described here assumes that voltage measurements are available only at the sending end. The procedure consists of three stages. In the first stage, the modal transformation is applied to the measured voltage signals. Clarke [8] transformation matrix is used as:

$$\begin{bmatrix} V_1 \\ V_2 \\ V_3 \end{bmatrix} = \frac{1}{\sqrt{3}} \begin{bmatrix} 1 & 1 & 1 \\ \sqrt{2} & -\frac{1}{\sqrt{2}} & -\frac{1}{\sqrt{2}} \\ 0 & \frac{\sqrt{3}}{\sqrt{2}} & -\frac{\sqrt{3}}{\sqrt{2}} \end{bmatrix} \cdot \begin{bmatrix} V_a \\ V_b \\ V_c \end{bmatrix}$$

where  $V_a$ ,  $V_b$  and  $V_c$  are phase voltages,  $V_1$  is ground mode voltage and  $V_2$ ,  $V_3$  are aerial mode voltages. In the second stage, the discrete wavelet transform (DWT) is applied to the modal voltages and the squares of the wavelet transform coefficients ( $WTC^2$ ) are obtained in order to determine the instant when the energy of the signal reaches its maximum value. Daubechies-4 [9] mother wavelet is used for wavelet transformation. Then in the final stage, ground mode  $WTC^2$ s in scale-1 are observed in order to determine the fault type (whether the fault is grounded or not) and aerial mode  $WTC^2$ s in scale-1 are processed based on the Bewley lattice diagram [10] of the fault initiated travelling waves in order to determine the fault location. In the following sections the last stage of the fault location procedure is described in detail for various possible cases.

## 3 Fault Location in Distribution Systems with DG



impacts of DGs considerably change depending on their location and size. It is known that an increase in generation capacity, increases the fault current. Thus, introduction of DGs to the radial distribution systems requires further study on existing protective device coordination and protection configuration. Furthermore, fault location problem in radial distribution systems, where only one end measurements are available, presents challenges due to the DG involvement in the distribution system. When a fault occurs, the fault current consists of not only the source current but also the DG current. There is an increase in fault current due to the increase in generation capacity, however there is a decrease in source current since the DG is also supplying the fault current. The decrease in source current leads a higher voltage at the measurement location. Since there is an increase in voltage and decrease in current, the impedance seen from the source location will be higher than the value obtained for the same fault conditions on the distribution system without DG. The impedance based fault location methods fail to locate the fault in such cases.

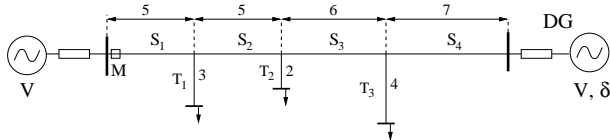


Figure 1: Studied distribution system with DG

The proposed fault location method first determines the type of the fault by observing the ground mode signal. Provided that the ground mode signal exists for only grounded faults, the proposed technique is developed accordingly. If the fault is ungrounded or balanced, there are no remote end reflections [6]. However for the grounded faults there are reflections of backward and forward travelling waves from all remote ends. Thus, the fault location procedure for grounded and ungrounded faults is described separately. In the following sections the details of the fault location method is described. The investigations based on Bewley diagrams of the various fault conditions are introduced. The distribution system with DG in Figure 1 is studied. The effect of the DG existence on the proposed fault location technique is also discussed.

### 3.1 Fault Location for Grounded Faults

Due to the multiple and superimposed reflections at the discontinuities, the Bewley diagrams of the grounded faults at different locations give complex travelling wave signatures at the measurement location. The backward and forward travelling waves arriving at the measurement point create different patterns depending on the location of the fault in the distribution system. The faults occurring on the intermediate sections cause more complex travelling wave patterns than those due to the faults occurring on the load branches.

First, the approximate faulted region is determined by comparing the time difference of initial peak arrival times of  $WTC^2$ s of aerial and ground mode voltages with those of the same distance but for different regions such as, one for intermediate section and other for load branch. After the region is identified, the exact fault location is calculated by using the procedures described in the following sections for intermediate sections and load branches.

and ground mode  $WTC^2$ s increases as the fault location moves far away from the measurement point. Once the approximate distance is predicted, the  $WTC^2$  pattern of the fault is compared with those obtained for the same distance but for different regions such as, one for intermediate section and other for load branch. After the region is identified, the exact fault location is calculated by using the procedures described in the following sections for intermediate sections and load branches.

#### 3.1.1 Faults on an Intermediate Section, $S_i$

Assume a grounded fault located in the first half of the section  $S_1$  as shown in Figure 2. The faulted half is identified by using the comparison of the time difference of initial peak arrivals of aerial and ground mode  $WTC^2$ s with the time difference,  $t_m$ , obtained for a fault in the middle of the line. If the time difference is smaller than  $t_m$ , the faulted region is identified as the first half and Equation (1) is used for fault location [6].

$$x = \frac{v \times \Delta t}{2} \quad (1)$$

$$\Delta t = t_2 - t_1$$

where  $v$  is the aerial mode velocity,  $t_1$  is the arrival time of the first peak of the aerial mode  $WTC^2$  corresponding to the backward travelling wave and  $t_2$  is the arrival time of the second peak of the aerial mode  $WTC^2$  corresponding to backward travelling wave reflected from fault point.

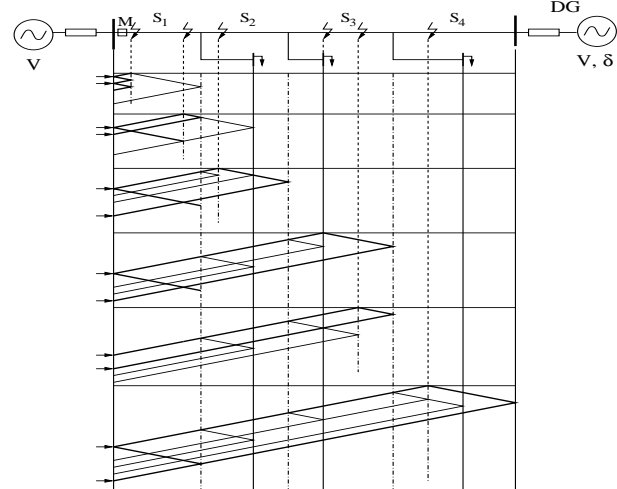


Figure 2: Bewley diagram for faults located at sections

If the time difference is larger than  $t_m$ , the fault is identified to be closer to the remote end as can be seen in Figure 2 and Equation (2) is used in order to calculate the distance [6].

$$x = \frac{\Delta t' \times v}{2} \quad (2)$$

$$\Delta t' = \frac{2 \times L}{v} - \Delta t$$

$$\Delta t = t_2 - t_1$$

time of the second peak of the aerial mode  $WTC^2$  corresponding to forward travelling wave reflected from the remote end and  $L$  is the total line length of  $S_1$ .

If the fault is at one of the other intermediate sections ( $S_2, S_3$  or  $S_4$ ), once the faulted region is identified using the time difference technique, Equation (3) is used for exact fault location. The arrival time,  $t_j$ , of the  $WTC^2$  peak corresponding to the reflected forward travelling wave increases as the fault location moves closer to the measurement point in the section. Assume a fault in  $S_3$ , closer to the measurement location as shown in Figure 2. The forward travelling wave, which is reflected from the remote end of the  $S_3$ , arrives at the measurement location as the fourth peak. However, the forward travelling wave arrives at the measurement location as the second peak for a fault closer to the remote end of  $S_3$ . The exact fault location is calculated using Equation (3).

$$x = \frac{\Delta t' \times v}{2} \quad (3)$$

$$\Delta t' = \frac{2 \times L_t}{v} - \Delta t$$

$$\Delta t = t_j - t_1$$

where  $v$  is the aerial mode velocity,  $t_1$  is the arrival time of the first peak of the aerial mode  $WTC^2$  corresponding to backward travelling wave,  $t_j$  is the arrival time of the  $j$ th peak of the aerial mode  $WTC^2$  corresponding to forward travelling wave reflected from the remote end and  $L_t$  is the total line length from the measurement point to the end of the faulted section. For a fault in  $S_3$ ,  $L_t = L_{S_1} + L_{S_2} + L_{S_3}$ .

### 3.1.2 Faults on a Load Branch, $T_i$

Depending on the length of the load branches, the arrival time of the forward travelling wave increases as the fault location moves closer to measurement location as shown in Figure 3.

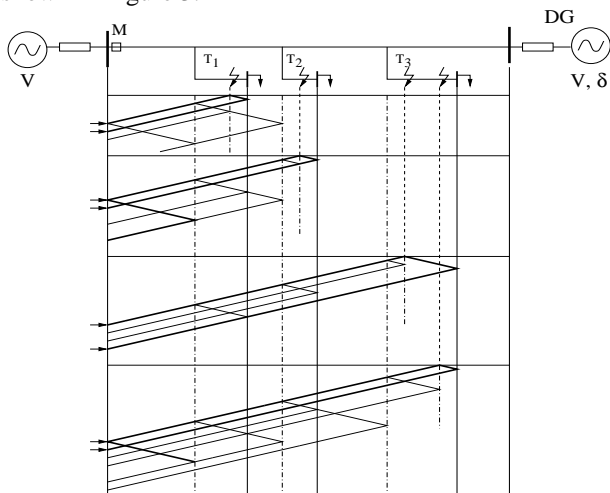


Figure 3: Bewley diagram for faults located at taps

Once the fault is identified in a load branch by using the time difference comparison of initial peak arrivals of  $WTC^2$  signals, the exact fault location is calculated using Equation (3). The procedure is not differ-

ent than the one for the intermediate sections, however the  $WTC^2$  patterns of faults at load branches are drastically different than those obtained for faults along intermediate sections.

### 3.2 Fault Location for Ungrounded/Symmetric Faults

Provided that there are no remote end reflections for the ungrounded faults, as shown in Figure 4 for an intermediate fault, the approximate region determination is based upon the aerial mode  $WTC^2$  patterns obtained for faults along the sections and along the load branches.

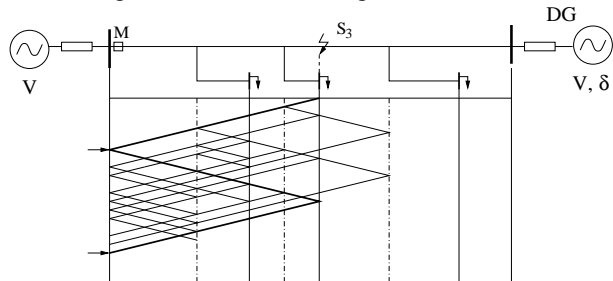


Figure 4: Bewley diagram for an ungrounded fault

Since there are significant discrepancies between the  $WTC^2$  patterns and magnitudes of intermediate faults and load branch faults, once the approximate region is determined, Equation (4) is used for fault location calculations utilizing the Bewley diagram.

$$x = \frac{v \times \Delta t}{2} \quad (4)$$

$$\Delta t = t_j - t_1$$

where  $v$  is the aerial mode velocity,  $t_1$  is the arrival time of the first peak of the aerial mode  $WTC^2$  corresponding to the backward travelling wave and  $t_j$  is the arrival time of the  $j$ th peak of the aerial mode  $WTC^2$  corresponding to backward travelling wave reflected from the fault point.

### 3.3 The effect of DG on Fault Location Procedure

The effect of a fault in distribution system on the main generation decreases due to the existence of DG. Thus, the severeness of the voltage transient recorded at the measurement location,  $M$ , is lessened. However, the pattern of the wavelet transform of the voltage signal remains same while the magnitude of the  $WTC^2$ s changes as shown in Figure 5 and Figure 6. Nevertheless, the change in magnitude is insignificant and unlike the power frequency based methods, the proposed fault location procedure is independent of the existence of distributed generation.

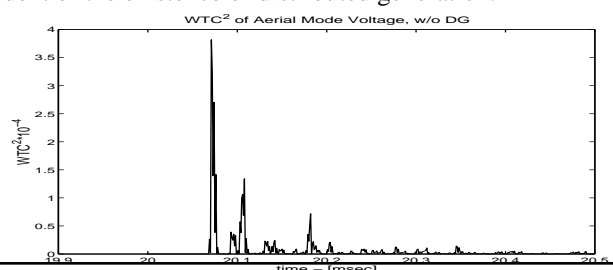


Figure 5: Aerial mode  $WTC^2$  s w/o DG for a fault 13 miles away from section  $S_3$

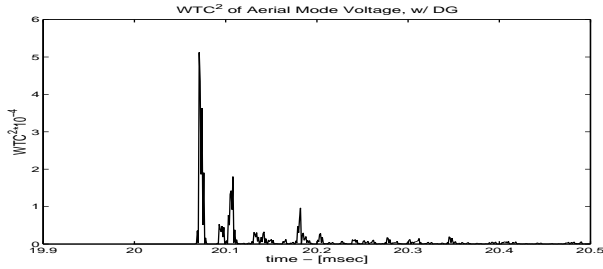


Figure 6: Aerial mode  $WTC^2$ s w/ DG for a fault 13 miles away from M in section  $S_3$

#### 4 Simulation Results

The transient simulations are carried out by using ATP/EMTP program. The results are processed in MATLAB by using Wavelet Analysis Toolbox. The tower configuration of a 10 kV distribution line is given in Table 1.

| Ph.               | 0    | 1     | 2     | 3     |
|-------------------|------|-------|-------|-------|
| Skin              | 0.5  | 0.5   | 0.5   | 0.5   |
| R [ $\Omega$ /mi] | 2.26 | .2797 | .2797 | .2797 |
| IX                | 4    | 4     | 4     | 4     |
| X                 | 0    | 0     | 0     | 0     |
| D [in]            | .621 | .741  | .741  | .741  |
| Hor. [ft]         | 0    | -3.66 | 0     | 3.66  |
| Vtower [ft]       | 33   | 28.5  | 28.5  | 28.5  |
| Vmid [ft]         | 33   | 28.5  | 28.5  | 28.5  |

Table 1: ATP Conductor and Tower Configuration Data for a 10 kV Distribution Line

Distributed parameter transmission line model is used. The line parameters are evaluated at 5000 Hz as well as the aerial mode and ground mode propagation velocities by using ATP LCC line constants routine. Ground mode propagation velocity,  $v_0$ , is calculated as 167300  $mi/sec$  while aerial mode propagation velocity,  $v_1$ , is calculated as 183837  $mi/sec$ . The sampling frequency is chosen as 1  $MHz$ . All the line segments are assumed to be fully transposed. The fault location algorithm is given as:

- Voltage measurements are recorded at one end.
- Modal transformation is applied to the measured voltages.
- DWT is applied to the modal and ground mode voltages.
  - If the ground mode is not zero;
    - \* Calculate the time difference of the arrival peaks of aerial and ground mode  $WTC^2$ s, and determine the approximate distance using the pre obtained time differences for various fault locations.
    - \* Use the pre-obtained  $WTC^2$  patterns to determine the region and

15th PSCC, Liege, 22-26 August 2005), if the fault is in first half of the first section

- use Equation (2), if the fault is in second half of the first section
- use Equation (3) otherwise.

– If the ground mode is zero;

- \* Use the pre-obtained  $WTC^2$  patterns to determine the approximate region and use Equation (4) for fault location

Assume a 1-phase-to-ground fault in  $T_3$ , 18 miles away from the measurement point. The time difference,  $\Delta t$ , between the initial peak arrivals of aerial and ground mode voltage  $WTC^2$ s for various faults in all sections are obtained as:

$$\Delta t = x_f \times \left( \frac{1}{v_0} - \frac{1}{v_1} \right) \quad (5)$$

where  $x_f$  represents fault location,  $v_0$  and  $v_1$  represent ground mode and aerial mode velocities respectively. Table 2 shows the calculated time difference,  $\Delta t$  for various fault locations. For the simulated fault, this time difference,  $\Delta t$ , is 9  $\mu s$  as shown in Figure 7. Hence, the faulted region is determined as either  $S_4$  or  $T_3$ .

| $x_f$ - [mi] | $\Delta t$ - [ $\mu sec$ ] | Section    |
|--------------|----------------------------|------------|
| 2.5          | 1.34                       | $S_1$      |
| 4            | 2.15                       | $S_1$      |
| 6            | 3.22                       | $S_2, T_1$ |
| 8            | 4.3                        | $S_2, T_1$ |
| 12           | 6.45                       | $S_3, T_2$ |
| 14           | 7.52                       | $S_3$      |
| 18           | 9.67                       | $S_4, T_3$ |
| 20           | 10.75                      | $S_4, T_3$ |

Table 2: Time differences of initial peak arrivals of aerial and ground mode  $WTC^2$ s for various fault locations

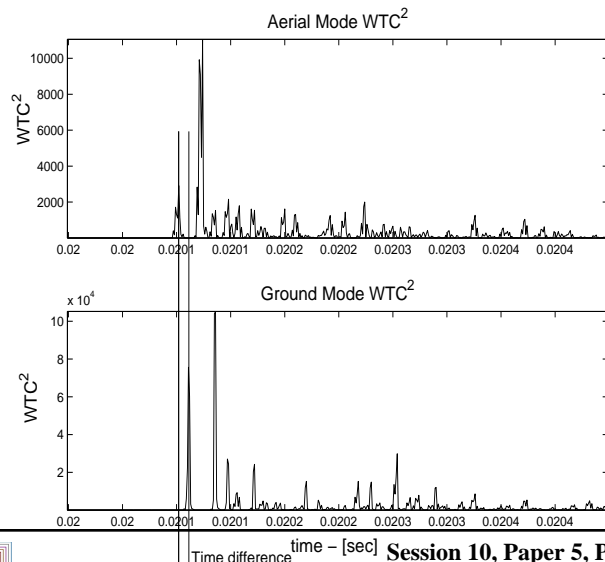
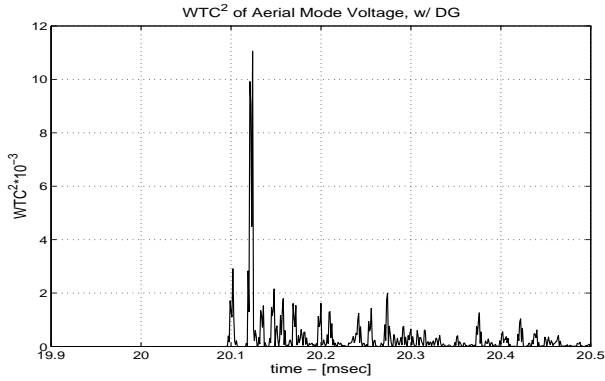
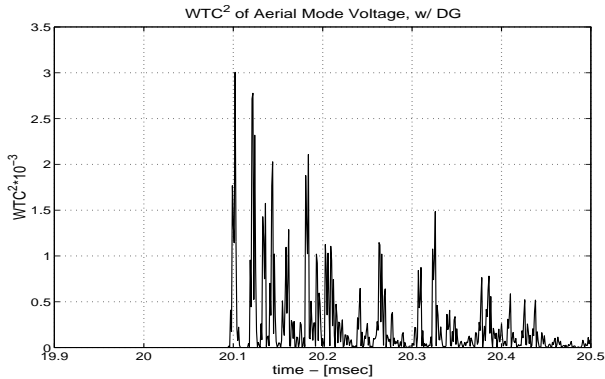


Figure 7: Aerial and ground mode  $WTC^2$ s w/ DG



**Figure 8:** Aerial mode  $WTC^2$ s w/ DG for a fault 18 miles away from  $M$  in section  $T_3$



**Figure 9:** Aerial mode  $WTC^2$ s w/ DG for a fault 18 miles away from  $M$  in section  $S_4$

In Figure 8 and in Figure 9 the  $WTC^2$ s of the aerial mode voltages are given for two faults located 18 miles away from the measurement point,  $M$  in  $T_3$  and in  $S_4$  respectively. The significant difference between the patterns is used to differentiate between faults occurring at the same distance from the substation but on either load branches or line sections. In this example, the observed pattern matches the one corresponding to that of a load branch and hence it is decided that the faulted branch is  $T_3$ . Thus, the location of the fault is determined using Equation (3) where the forward travelling wave reflected from the remote end of  $T_3$  arrives at  $M$  as the second peak and the time difference,  $\Delta t_{21} = t_2 - t_1$  between two consecutive peaks of aerial mode  $WTC^2$ s as shown in Figure 8 is  $22 \mu\text{sec}$ . Details of the calculations are shown below:

$$x_f = \frac{183837}{2} \times \left( \frac{2 \cdot L_T}{183837} - 22 \cdot 10^{-6} \right) = 17.98 \text{ mi}$$

$$L_T = S_1 + S_2 + S_3 + T_3 = 20 \text{ mi}$$

where  $L_T$  is the total line length from the measurement point,  $M$ , to the end of the faulted branch.

## 5 Conclusions

This paper proposes a travelling wave based fault location method to be used in distribution systems with distributed generation. The main advantage of the proposed

approach is its insensitivity to naturally occurring infeed from the distributed generators during a fault. Such infeed is typically unpredictable and makes the impedance based conventional fault location methods vulnerable to errors. Furthermore, the proposed approach has the added advantage of requiring fault signals only from the substation end of the distribution feeder. Simulation results are provided to illustrate some of these benefits on a test system.

## REFERENCES

- [1] A. Girgis and S. Brahma, *Effect of distributed generation on protective device coordination in distribution system*, Large Engineering Systems Conference on Power Engineering, July 2001, pp. 115 - 119
- [2] C.W. So and K.K. Li, *Protection relay coordination on ring-fed distribution network with distributed generations*, IEEE Region 10 Conference on Computers, Communications, Control and Power Engineering, Vol.3, Oct. 2002, pp. 1885 - 1888
- [3] M.T. Doyle, *Reviewing the impacts of distributed generation on distribution system protection*, IEEE PES Summer Meeting, Vol.1, July 2002, pp. 103 - 105
- [4] Z.Q. Bo, G. Weller and M.A. Redfern, *Accurate fault location technique for distribution system using fault-generated high-frequency transient voltage signals*, IEE Proceedings on Generation, Transmission and Distribution, Vol.146, No. 1, Jan. 1999, pp. 73 - 79
- [5] Z. Xiangjun, K.K. Li, W.L. Chan, S. Sheng, *Multi-agents based protection for distributed generation systems*, IEEE International Conference on Electric Utility Deregulation, Restructuring and Power Technologies, Vol.1, April 2004, pp. 393 - 397
- [6] F.H. Magnago and A. Abur, *Fault Location Using Wavelets*, IEEE Transactions on Power Delivery, Vol. 13, No. 4, Oct. 1998, pp. 1475-1480.
- [7] C.Y. Evrenosoglu and A. Abur, *Travelling Wave Based Fault Location for Teed Circuits*, IEEE Transactions on Power Delivery, in press
- [8] E. Clarke, *Circuit Analysis of AC Power Systems, Symmetrical and Related Components*, John Wiley & Sons, NY, 1943
- [9] I. Daubechies, *Ten Lectures on Wavelets*, SIAM, Pennsylvania, 1992
- [10] L.V. Bewley, *Travelling Waves on Transmission Systems*, John Wiley & Sons, NY, 1951